

Small-scale transport of trace elements Nb and Cr during growth of titanite: an experimental study at 600 °C, 0.4 GPa

Friedrich Lucassen · Gerhard Franz ·
Dieter Rhede

Received: 18 March 2012 / Accepted: 28 July 2012 / Published online: 15 August 2012
© Springer-Verlag 2012

Abstract Trace element distribution in titanite overgrowths on rutile has been investigated experimentally at 600 °C, 400 MPa and f_{O_2} near NiNiO buffer. Compositionally homogenous Cr- or Nb-doped synthetic rutile single crystals or Nb-containing natural rutile crystals were the source of Cr, Nb and Ti to synthesize titanite using the double-capsule technique. All element exchange with the source of Si, Ca and Al occurred via a NaCl–H₂O fluid. Titanite forms quickly and exclusively around the rutile crystals. The titanite overgrowth separates rutile from the bulk fluid, and all elements from rutile dissolution have to pass through the titanite rim. Trace element concentrations in titanite show a considerable scatter in experiments with and without Al, although the average concentrations of Cr or Nb of titanite around compositionally homogeneous synthetic rutile approach the expected values for closed system conditions. Variability of Al with Cr or Nb in the

titanite is not correlated. The Al zoning is irregular and patchy, and also the distribution of trace elements does not show systematic trends in the spatial distribution. In experiments using zoned natural rutile, the concentrations of Nb in titanite are related to the Nb zoning in rutile, but the contents also vary unsystematically. Under the controlled conditions of the experiment, the explanation for the strongly irregular spatial distribution is most likely due to variations in elemental concentrations during transport from the rutile along the titanite grain boundaries. The transport pathway is complex because grain boundary migration is important during titanite growth. Such irregular element distribution is also found in a natural sample of titanite overgrowth on rutile from an eclogite with retrograde overprint in the amphibolite facies. Transport of Ti and trace elements was focused on grain boundaries and shielded from the rutile as a source of these elements. We conclude that this type of zoning is not related to changes in P – T or composition in an open system, but solely controlled by transport in and through the titanite rim.

Communicated by J. Hoefs.

Electronic supplementary material The online version of this article (doi:10.1007/s00410-012-0784-y) contains supplementary material, which is available to authorized users.

F. Lucassen · G. Franz
Technische Universität Berlin, Fachgebiet Petrologie-ACK 9,
Ackerstr. 71–76, 13355 Berlin, Germany

F. Lucassen (✉)
Isotope Geochemistry Group, Department
of Geosciences, MARUM Center for Marine
Environmental Sciences, University of Bremen,
Postfach 330 440, 28334 Bremen, Germany
e-mail: Lucassen@uni-bremen.de

D. Rhede
Deutsches GeoForschungsZentrum, Telegrafenberg,
14473 Potsdam, Germany

Keywords Titanite growth on rutile · Cr and Nb in rutile · Cr and Nb in titanite · Experimental study

Introduction

Trace elements in metamorphic and igneous rocks can be hosted by single or few accessory minerals with high partition coefficients for the respective elements (e.g., Bea et al. 2006). Release and redistribution of trace elements occur if the host mineral becomes unstable and reacts due to changes in physical and/or chemical parameters in the rock. Mineral reactions and hence redistribution (transport) of trace (and major) elements are largely enhanced by

mobile fluid phases during devolatilization of volatile-rich rocks during prograde or the reverse process in dry rocks during retrograde metamorphism (e.g., Fyfe et al. 1978). Mobility of trace elements triggered by metamorphic reactions potentially influences a broad spectrum of applications of such elements in metamorphic petrology and geochemistry. The knowledge of trace element composition and distribution in minerals evolved rapidly with the progress of in situ analytical methods and proliferation of analytical equipment (e.g., Kohn 2003; Bea et al. 2006; Storey et al. 2007; Martin 2009; Smith et al. 2009). Trace element compositional zoning of minerals has been extensively studied in melt–mineral systems to monitor changing melt compositions. In metamorphic minerals, studies of trace element compositional zoning were motivated by the application of trace element geothermobarometry (e.g., Zr in rutile and titanite; Zack et al. 2004; Hayden et al. 2008), in situ isotopic dating (e.g., Grew et al. 2008; Smith et al. 2009), or mineral–mineral (fluid) interaction (e.g., Schmidt et al. 2009; Martin 2009; Lucassen et al. 2010a, 2011). Compositional zoning of minerals reflects either changing physicochemical conditions during mineral growth (growth zoning) or compositional modifications during the post-growth history by volume diffusion in the mineral. In natural minerals under high-*T* conditions, diffusion patterns commonly overprint growth zoning, leading to the formation of complex element distribution pattern (e.g., Konrad-Schmolke et al. 2007). The motivation for our experimental study is to show that during growth of a metamorphic mineral at fixed *P–T*, a complex and irregular appearing distribution pattern of trace elements can be formed.

Titanite is considered as a versatile sink for various trace elements (e.g., Ribbe 1980; Oberti et al. 1991). Substitution on the ^{vii}Ca site includes rare earth elements, Y, Sr, U, Th, Pb and Fe²⁺. Niobium, Ta, Zr, W (HFSE, high-field strength elements), Cr, Fe³⁺ and Al substitute on the ^{vi}Ti site, OH and F substitute on the O1 site, whereas the ^{iv}Si site is not affected at crustal pressures. High concentrations of trace elements occasionally reported from titanite suggest that their incorporation is controlled by availability rather than compatibility, for example, Ta₂O₅ and Nb₂O₅ in pegmatitic titanite with 6 and 5 wt%, respectively (Groat et al. 1985); Nb₂O₅ up to ~10 wt% in metamorphic titanite (Bernau and Franz 1987). The commonly observed variation of major element composition in natural titanite is dominated by up to 0.5 atoms pfu substitution of (Al³⁺, Fe³⁺) + (F⁻, OH⁻) ↔ Ti⁴⁺ + O²⁻ (e.g., Oberti et al. 1991).

Growth of titanite on rutile up to complete consumption of the latter is observed in many retrogressed metamorphosed mafic rocks (e.g., Brewer et al. 2003; Romer and Rötzler 2003; Lucassen et al. 2011). Rutile is the prevailing

Ti accessory mineral at high pressures in amphibolite and granulite facies and in eclogite facies rocks of mafic bulk compositions. The rutile hosts most of the Nb and Ta contents in these rocks and can also contain elements such as W, Zr, Cr and V in appreciable amounts (e.g., Zack et al. 2002; Meinhold 2010 and references therein). Towards lower *T* and *P* and increasing fluid activity, the accessory Ti mineral titanite is stable (e.g., Frost et al. 2000).

We investigated experimentally the Nb and Cr distribution in titanite during growth in the dissolution–precipitation reaction $\text{TiO}_2(\text{rutile})_{\text{in fluid}} + \text{CaSiO}_3(\text{wollastonite})_{\text{in fluid}} = \text{CaTiSiO}_5(\text{titanite})$, the latter forming an overgrowth on the rutile single crystal. The possible influence of the substitution of Ti by Al on the trace element distribution was also studied at the same *P–T* conditions of 400 MPa/600 °C, which are in the stability field of titanite for given bulk compositions at temperature in the amphibolite facies. Our experiments mimic a scenario that includes transport of Ca, Si (and optional Al) by a fluid phase (H₂O, NaCl and optional F) towards rutile. The trace elements Nb and Cr are available during dissolution of rutile, the only source of Ti and the trace elements Nb or Cr. Wollastonite (+Al₂O₃) or grossular (instead of wollastonite and Al₂O₃) serves as Ca, Si (+Al) source. During the experiment, rutile is separated from the Ca, Si and Al sources by a permeable Pt capsule and all elemental transport within the capsules occurs via the fluid. We will show that the contents of Nb and Cr in newly formed titanite as rims around rutile is variable and irregularly distributed, because Nb and Cr released from the rutile are not homogenized by the fluid. Similarly as Ti, they remain in close vicinity of their source.

Experimental approach, starting materials and analytical technique

Experimental approach

All experiments were performed with the same double-capsule technique (see electronic appendix eFigure 1) at 600 °C and 400 MPa in cold seal autoclaves using water as a pressure medium. The *f*_{O₂} is fixed close to NNO by the use of Ni reducers in the autoclave assemblage. Detailed account to the experimental technique is given in Lucassen et al. (2010b, 2012) where we investigated the zoning pattern Al–Ti in synthetic titanite and the reaction morphology at the titanite–rutile interface. For all runs with natural rutile as a starting material, we had used Pt capsules for the inner capsule; for most runs with synthetic rutile and Fe-bearing grossular, we used Au or AgPd capsules.

Key information of the experimental setup is given in Table 1. Minimum run time was 14 days; we had shown

Table 1 Run data for the experiments at constant P – T conditions of 400 MPa and 600 °C

| Run | Run time (days) | Rutile (g) | Wollastonite (g) | Al ₂ O ₃ (Al) or grossular (grs) (g) | CaF ₂ (g) | SiO ₂ (quartz) (g) | H ₂ O + NaCl* (g) |
|--------------------------------------|-----------------|------------|------------------|--|----------------------|-------------------------------|------------------------------|
| <i>Natural rutile</i> | | | | | | | |
| RT11 | 30 | 0.0487 | 0.0592 | | | | 0.0557 |
| RT16** | 60 | 0.0599 | 0.0591 | 0.0305 (Al) | | | |
| RT17** | 60 | 0.0553 | 0.0412 | 0.0209 (Al) | 0.0096 | | 0.1467 |
| RT20** | 107 | 0.0524 | 0.0533 | 0.0329 (Al) | 0.0128 | | 0.1133 |
| RT21 | 107 | 0.0287 | 0.0622 | | | | 0.1148 |
| RT22** | 30 | 0.0640 | 0.0462 | 0.0385 (Al) | | | 0.1224 |
| <i>Synthetic 2,000 µg/g Cr-doped</i> | | | | | | | |
| RT41 | 30 | 0.0117 | 0.0220 | 0.0750 (Al) | 0.1158 | 0.0894 | 0.0956 |
| RT42 | 14 | 0.0121 | | 0.0206 (grs) | | | 0.1007 |
| RT50 | 14 | 0.0048 | | 0.0134 (grs) | | 0.0089 | 0.0833 |
| RT51 | 14 | 0.0051 | | 0.0208 (grs) | | | 0.1416 |
| <i>Synthetic 500 µg/g Nb-doped</i> | | | | | | | |
| RT49 | 14 | 0.0061 | | 0.0106 (grs) | | | 0.1432 |
| RT69 | 30 | 0.0042 | | 0.0075 (grs) | | 0.0054 | 0.0990 |
| RT74 | 30 | 0.0058 | | 0.0089 (grs) | 0.0035 | 0.0046 | 0.0550 |

* The fluid contains ~50 wt% NaCl except run RT11 with 20 wt% NaCl; ** Run data RT16, RT17, RT20 and RT22 from Lucassen et al. (2010b)

previously that after this time, no significant changes occur in the growth of the reaction rim (Lucassen et al. 2012). In the experiments, the bulk composition and the phases in the outer capsule were varied: first, we used wollastonite (size between ~100 and 500 µm) as Ca–Si source in the system TiO₂–CaO–SiO₂ fluid. The system was then extended by γ -Al₂O₃ to account for possible influence of major element variability in titanite on the trace element incorporation. The bulk composition of wollastonite + γ -Al₂O₃ closely corresponds to that of grossular, which was also used (grain size between ~100 and 500 µm) to check for possible influence of different solubility of the Ca–Al–Si source. These systems are SiO₂-undersaturated, but Al-saturated. Some experiments in the TiO₂–CaO–SiO₂–Al₂O₃ fluid system were run under SiO₂-saturation by adding natural quartz (size ~500 µm). Exploratory experiments showed that solubility of the crystalline phases in H₂O is low and hence reaction progress slow. Therefore, we added Cl and in some experiments additional F to the aqueous fluid, because solubility of rutile (e.g., Ayers and Watson 1993; Antignano and Manning 2008; Rapp et al. 2010), grossular (Fockenberg et al. 2008), wollastonite, corundum and quartz (Newton and Manning 2006) is strongly enhanced. The extrapolation of solubility from simple mineral-fluid studies to the more complex solute in our experiments is likely not straightforward, but the observations of enhanced titanite growth in Cl- and F-bearing fluids indicate

enhanced solubility in accordance with solubility studies (*cf* references above).

Starting material

Experiments were carried out with both natural and synthetic rutile. Niobium or Cr-doped synthetic rutile was grown by the flame fusion (Verneuil) method from near pure TiO₂ (provider: SurfaceNet GmbH, Rheine, Germany). Trace element contents in rutile and their distribution were checked before and after run by electron microprobe analysis (EMP) and laser ablation inductively coupled mass spectrometry (LA-ICP-MS; for the applied technique see Lucassen et al. 2010a, 2011). In individual EMP analyses with a beam size of 1–2 µm and the corresponding excitation volume, the Nb contents in the crystals vary between 330 and 610 µg/g (rutile before reaction) or 420–620 µg/g (rutile from runs RT69 and RT74), but is more uniform between 460 and 512 µg/g (rutile before reaction) in LA-ICP-MS analyses. The time-resolved spectra show no relation of the calculated ⁹³Nb intensities to spot size (60, 44 and 32 µm diameter) or depth (time), and Nb distribution in the rutile is uniform at this scale of measuring. The average Nb contents of the rutile from EMP (505 ± 80 µg/g, $n = 30$; unreacted rutile; 498 ± 56 µg/g; $n = 48$, rutile runs RT69 and RT74) and LA-ICP-MS (480 ± 19 µg/g, $n = 22$) are similar. The Cr

content is uniform with $\sim 2,000$ $\mu\text{g/g}$ (EMP range, 1,910–2,100 $\mu\text{g/g}$; average, $2,016 \pm 42$ $\mu\text{g/g}$; $n = 30$; LA-ICP-MS range, 1,950–2,144 $\mu\text{g/g}$; average, $2,010 \pm 43$ $\mu\text{g/g}$; $n = 21$).

Natural rutile is from a pegmatite in Minas Gerais, Brazil. X-ray powder diffraction analysis (XRD) as well as optical microscopy showed that it is free of other phases such as ilmenite or hematite (Lucassen et al. 2010b), but it shows sector zoning. In difference to the synthetic rutile, the trace element distribution in the natural rutile is heterogeneous. Niobium contents are highly variable (~ 500 – $2,500$ $\mu\text{g/g}$) and roughly correlated with variable Fe contents ($\sim 3,000$ – $9,500$ $\mu\text{g/g}$) in the sectors (see eFigure 2 in the electronic appendix). Analyses of three small rutile fragments by solution ICP-MS reveal also variable amounts of Nb (805; 955; 2,040 $\mu\text{g/g}$), Ta (200; 280; 180 $\mu\text{g/g}$) and W (2,300; 3,100; 2,700 $\mu\text{g/g}$); Zr is <30 $\mu\text{g/g}$.

The natural grossular used in some experiments as the Ca, Si and Al source ($\text{Ca}_{2.86} \text{Fe}_{0.07}^{2+} \text{Mg}_{0.07} \text{Fe}_{0.10}^{3+} \text{Al}_{1.90} \text{Si}_{3.00} \text{O}_{12}$) is the same that was used in a solubility study by Fockenberg et al. (2008). Wollastonite is pure CaSiO_3 (Lucassen et al. 2010b) from a contact metamorphic rock from Namibia. Rutile and wollastonite were cleaned in HNO_3 and HCl , respectively; Au and Pt capsules were boiled in HNO_3 . The other ingredients are NaCl , $\gamma\text{-Al}_2\text{O}_3$ and CaF_2 (all analytical grade powders) and distilled H_2O .

Analytical technique

Titanite overgrowth of all samples was documented by SEM using a Hitachi S-2700 at TU-Berlin or a Zeiss Ultra 55 Plus at GFZ-Potsdam. The compositions of quench material on the surface of the titanite, new crystals in the outer capsule and the inner walls of the capsule were controlled by energy dispersive analysis. Chemical compositions of minerals in polished grain mounts were analysed by wavelength-dispersive analysis with a Cameca SX 100 EMP at the Deutsches GeoForschungsZentrum at operating conditions of 15 kV accelerating potential, 20 nA beam current and beam diameters of 1–2 μm . Peak counting times were 10–30 s, and backgrounds were counted 5–15 s. Standards were the following synthetic and natural minerals: topaz (F), albite (Na), orthoclase (Al, Si), borazite (Cl), wollastonite (Ca), rutile (Ti) and hematite (Fe). The raw intensity data were corrected with the ‘PAP’ program (Pouchou and Pichoir 1985). For trace element analysis, conditions were an accelerating voltage of 15 kV, a beam current of 100 nA, a beam size of 1 μm and counting times of 300 s on the peak. The following standards were used: synthetic Cr_2O_3 for Cr, Nb metal, orthoclase for Al and hematite for Fe. Fixed values for the major elements were included in the correction procedure.

The detection limit was ~ 50 $\mu\text{g/g}$ for Nb, ~ 45 $\mu\text{g/g}$ for Cr and 40 $\mu\text{g/g}$ for Fe. In the trace element measuring routine, Al (applicable in Al-bearing compositional systems) and/or Fe (applicable in runs with natural rutile and/or grossular) were analysed together with the trace elements Cr and Nb in order to evaluate the impact of major element (Al) variability. The contact between rutile and titanite is well defined, and the Al content in titanite and the Fe content in natural rutile are also used to identify mixed analyses in profiles.

The element mappings on polished sections of grain mounts in epoxy resin were carried out in the wavelength-dispersive mode with a Cameca SX100 and a JEOL JXA-8500F (HYPERPROBE) (a) moving the stage in steps of 0.1–2 μm , using a beam current of 40 nA, a focussed beam and counting times of 300–500 ms per step, or (b) scanning the focussed beam in steps of 0.04 μm and a counting time of 2 ms and 20 accumulations per frame.

Pattern of titanite growth on rutile

The appearance and morphology of titanite overgrowths on rutile have been previously documented in detail (Lucassen et al. 2010b, 2012). Complete or almost complete overgrowth of the rutile by titanite occurs already after 1-day runtime in both systems without and with Al or SiO_2 saturation (Table 1). With increasing runtime, small titanite crystals recrystallize to larger prismatic crystals and euhedral crystals grow into the fluid. There is no systematic difference of titanite overgrowth pattern between synthetic and natural rutile. Natural rutile additionally shows titanite growth in fractures invading or crosscutting the host rutile crystals. Fractured and unfractured rutile crystals occur within the same run and there is no difference in the composition of titanite growing on fractures or as rim around rutile.

Major element composition

In the system $\text{TiO}_2\text{--CaO--SiO}_2\text{--NaCl--H}_2\text{O}$, the only newly formed mineral in the experiments is titanite as a reaction rim around rutile. In the experiments with $\gamma\text{-Al}_2\text{O}_3$, the newly formed minerals are titanite around synthetic or natural rutile, and additionally grossular, anorthite and corundum in the outer capsule. The stable paragenesis at 600 °C/400 MPa for the system $\text{TiO}_2\text{--SiO}_2$ (saturated)– $\text{CaO--Al}_2\text{O}_3\text{--NaCl--H}_2\text{O}$ calculated with Perplex (Connolly 1990, 2009) is titanite–grossular–anorthite–wollastonite. This is consistent with the observed mineral assemblage, although we cannot account for the solid solution of Al, F, OH in titanite (see discussion in Tropper and Manning

2008). All starting materials are still present after the experiments except γ -Al₂O₃ that forms crystals of corundum already in 1-day experiments. We observed extensive precipitation of new wollastonite ('fluid-transport crystals') in the outer capsule from wollastonite dissolution in some experiments, but also transport crystals of quartz and corundum in respective starting compositions. The presence of Al leads to irregular, patchy zoning of the coupled Al–Ti–(OH, F) contents in the otherwise stoichiometric titanite as shown previously (Lucassen et al. 2010b). Considerable scatter of the Al–Cr and Al–Nb contents is observed in all runs (Fig. 1). The irregular pattern of the zoning is neither related to the Al source (γ -Al₂O₃ or grossular) nor the presence of F, SiO₂-saturation or SiO₂-undersaturation, or the use of natural or synthetic rutile. The effect of SiO₂-saturation is lowering the Al contents of titanite, with the lowest values in the F-free system and higher values in the presence of F, whereas Al₂O₃-saturation (SiO₂-undersaturation) extends the Al substitution in titanite (Fig. 1), which reaches up to 0.5 pfu of Al if F is present (Lucassen et al. 2010b). The zoning is controlled by the activity of Al at the site of titanite growth and not by *P* and *T* (Lucassen et al. 2010b).

Quench products appear as spheres or thin layers of porous microcrystalline (?) material of variable outline on the titanite. Quench contains variable proportions of Si, Ca, Al (in respective bulk compositions) and Na. Titanium is absent, below ~1 mol%, estimated from energy dispersive analysis and also not detected in quench or run products of the outer capsule (newly formed wollastonite and grossular garnet; Lucassen et al. 2010b). Rarely corundum occurs as a quench phase.

Trace element distribution in titanite

Cr- and Nb-doped synthetic rutile

Experiments with synthetic rutile were performed in the Al-bearing system (Table 1). The scatter of Cr and Nb (Fig. 1) contents in titanite is large, and the variation shows no systematic spatial distribution in 2D sections. Variation of Cr contents along profile lines and scattered single analysis is very similar with most points between 600 and 800 $\mu\text{g/g}$ (for frequency distribution, see eFigure 3 in the electronic appendix). Several analyses show Cr contents much higher than 800 $\mu\text{g/g}$ up to ~5,100 $\mu\text{g/g}$ that exceed the contents of the Cr source, but also much lower down to 240 $\mu\text{g/g}$. Chromium and Nb contents are not correlated with the Al contents of titanite (Fig. 1d). Distribution of Nb contents especially in runs RT49 and 74 shows a large scatter including a considerable number of analyses with Nb > 500 $\mu\text{g/g}$, which is the average content of the rutile

source. Extreme Nb concentrations reach ~7,000 $\mu\text{g/g}$. BSE images and small-scale X-ray mapping did not show indications for the presence of inclusions of Cr or Nb phases in titanite (Fig. 1).

Natural rutile

In the system without Al, Nb distribution in rutile and titanite was analysed along 17 profiles, and in the Al-bearing system along 18 profiles (representative profiles see Fig. 2a, for full data set see eFigure 4 in the electronic appendix) including the rutile. This analytical approach was chosen because Nb contents of rutile (combined with Fe; Fig. 2b, d) show strong zoning. The scatter of the Nb contents in titanite is large (Fig. 2). In most profiles, the average Nb content in titanite adjacent to rutile is substantially lower than in rutile (Fig. 3). There is a tendency that higher Nb contents in rutile at the rutile–titanite interface cause higher Nb contents in adjacent titanite in the same run, which means at least partial local control of Nb contents in titanite by the variable rutile composition. The Nb contents of Al-free and Al-bearing titanite are similar (Fig. 3) and there is no obvious correlation between Nb and Al.

Discussion

The synthetic, Cr- or Nb-doped rutile serves as a compositionally homogeneous model source in the evaluation of trace element incorporation from rutile into titanite. The average Cr and Nb contents of synthetic rutile are ~2,000 and ~500 μg , respectively, as measured by EMP and LA-ICPMS analyses. Though the EMP analyses of Nb-doped rutile indicate a larger scatter of Nb contents than LA-ICPMS analyses, both methods result in the same average Nb concentrations. Even neglecting the effect of averaging potential small-scale heterogeneities of Nb by the reaction, the scatter of Nb contents in the titanite exceeds the scatter observed in the EMP data of the rutile.

In our experiments, the rutile crystal (natural or synthetic) is the source of Ti and the trace elements Cr and Nb. Except titanite no other new Ti-bearing mineral formed in the experiments. Loss of these elements into the capsule material is unlikely, because we see no systematic effects of different capsule material (Pt or Au) on Cr or Nb contents of titanite as seen for Fe (van der Laan and van Groos 1991) and conclude that these elements do not alloy. The composition of quench material, the absence of Ti minerals in the outer capsule and the composition of newly formed minerals in the outer capsule (Lucassen et al. 2010b) indicate that the aqueous fluid in the outer capsule contains Ca, Si, Na, Cl (plus Al and F in respective compositions), but no traceable Ti (+Nb, Cr). This fluid is considered as

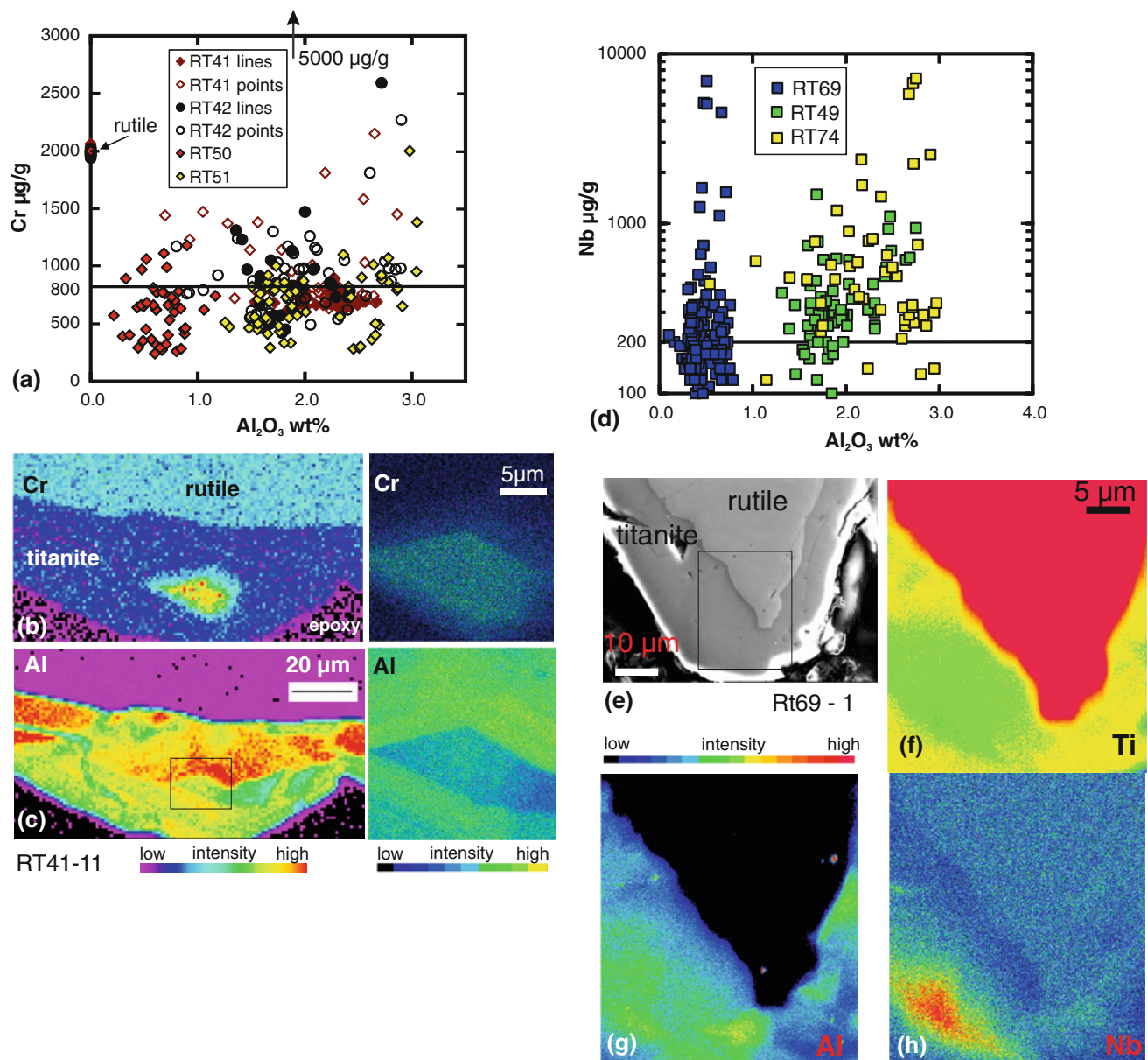


Fig. 1 Titanite composition around doped synthetic rutile **a, b, c** Cr and **d, e, f, g, h** Nb. **a** Cr–Al; the line at 800 $\mu\text{g/g}$ indicates the composition of titanite if all Cr from the dissolved rutile ($\sim 2,000$ $\mu\text{g/g}$) enters the titanite and is uniformly distributed. Random single point analyses and analyses along lines across the titanite (runs RT41 and RT42) show a similar scatter, although it seems more likely to encounter extreme values in random single points. Run RT 50 was at quartz saturation. **b, c** The Cr and Al distribution in low (*left column*)

and high-resolution (*right column*) element distribution maps; the area covered by the high-resolution maps is indicated by the *box* in (**c**). **d** Nb–Al; many analyses show a higher concentration than the expected composition of 200 $\mu\text{g/g}$ from the dissolved rutile (~ 500 $\mu\text{g/g}$) and some even higher than the Nb contents of the rutile (note log-scale). Run RT 69 was at quartz saturation. **e** Scanning electron microscope image of the titanite overgrowth on rutile of RT69. The *box* indicates the position of high-resolution mapping in (**f, g, h**)

the bulk fluid. The bulk of the Ti (+Nb, Cr) is transported through the reaction rim around the rutile, but not further. All Ti and trace elements released from the rutile are available.

The reaction progress is based on dissolution of the minerals providing the elements for the formation of titanite. The observation that titanite exclusively formed around rutile proves the relative immobility of Ti compared

with Ca, Si and Al. Dissolution of synthetic rutile should result in uniform trace element composition of the solute, that is, in the same Ti/Cr or Ti/Nb ratios independent of the spatial focus of dissolution on the rutile surface. If all Ti and Cr or Nb released from a rutile of uniform composition are incorporated and uniformly distributed in new titanite, the trace element contents from the rutile are diluted according to the ratio of the molecular weights rutile/

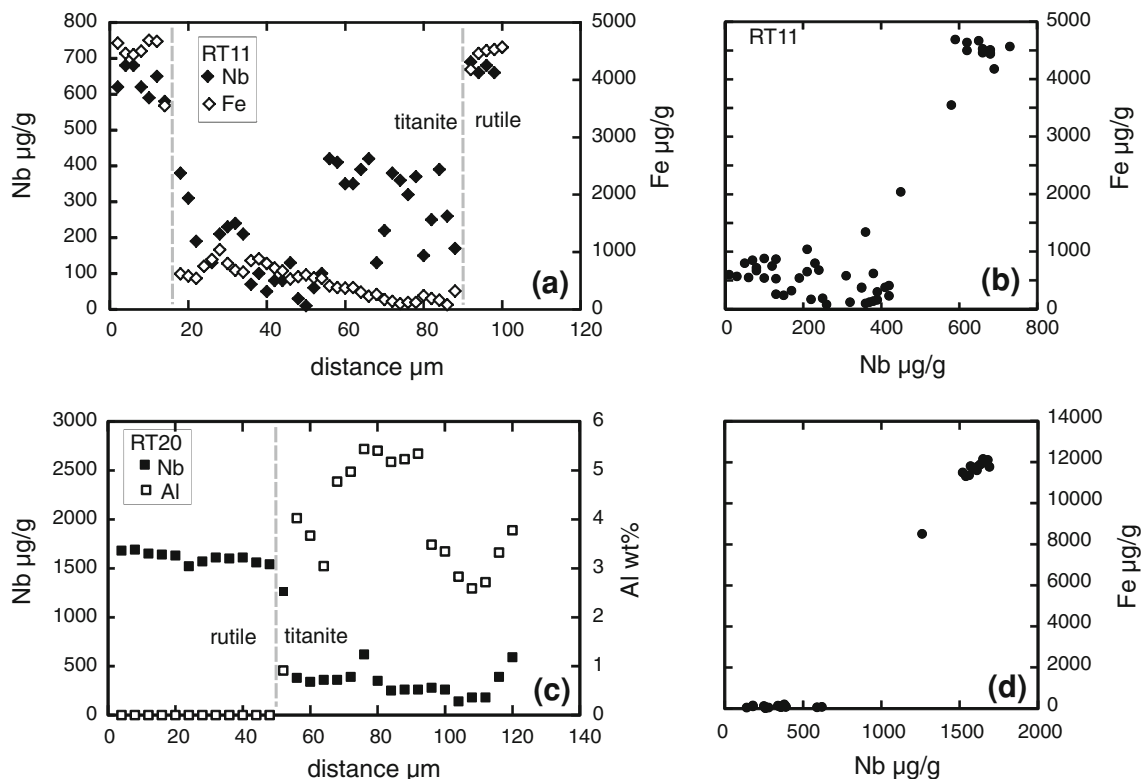


Fig. 2 a, b, c, d Examples of trace element content along profiles in titanite (natural Nb-bearing rutile as starting material). The profiles perpendicular to the rutile–titanite interface extend into rutile to check

for the local composition. a, b compositional system without Al, c, d compositional system with Al. Mind the different scales of the left and right ordinate in (a) and (c)

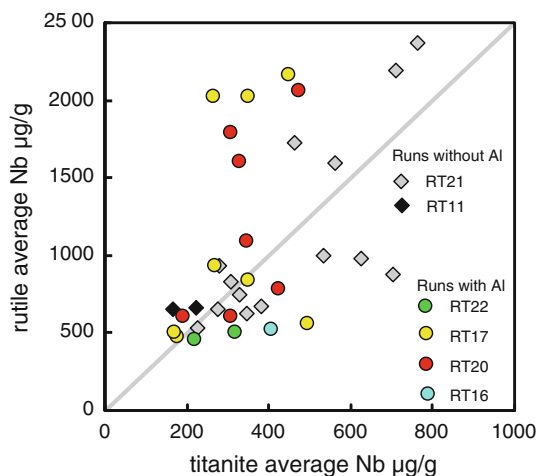


Fig. 3 Average Nb content of rutile and titanite calculated for individual profiles from experiments using natural rutile as starting material. The reference line represents a ratio of Nb in rutile/Nb in titanite of 1/2.5 according to the ratio of the molar masses of rutile/titanite

titanite of $\sim 1/2.5$, for example, the average contents of 2,000 $\mu\text{g/g}$ Cr or 500 $\mu\text{g/g}$ Nb in the synthetic rutile should result in 800 $\mu\text{g/g}$ Cr, respectively, 200 $\mu\text{g/g}$ Nb in the new titanite provided the spatial distribution of the trace elements in titanite is uniform. The latter values serve as

potential baseline composition in the discussion of trace element heterogeneity of the titanite. In contrast to the rutile source, the spatial distribution of Cr and Nb in the titanite is very heterogeneous (Fig. 1) and in addition contains small areas with high concentrations of Cr or Nb. High-resolution element mapping by EMP showed no indications for the presence of inclusions of Cr- (Fig. 1b, c) or Nb-rich (Fig. 1f–h) phases.

The average Cr content of titanite including all analyses is close to the theoretical value of $\sim 800 \mu\text{g/g}$ in runs RT41, RT42 and RT51 but considerably lower in RT50 (Table 2). If values above 1,000 $\mu\text{g/g}$ are excluded (corresponding to a 25 % overstep of the theoretical value), the average values are $\sim 740 \mu\text{g/g}$ (RT42), $\sim 720 \mu\text{g/g}$ (RT41), $\sim 650 \mu\text{g/g}$ (RT51) and $\sim 560 \mu\text{g/g}$ (RT50), about ~ 8 to ~ 30 % lower than the theoretical Cr concentration. Sequestration of Cr in the high Cr areas could be responsible for the missing Cr and we assume that Cr from the rutile is almost quantitatively included in the titanite.

The average Nb content (including analyses $\leq 250 \mu\text{g/g}$ allowing for a maximum of 25 % overstep of the theoretical Nb value of 200 $\mu\text{g/g}$) is $\sim 200 \mu\text{g/g}$ (RT49), $\sim 190 \mu\text{g/g}$ (RT74) and $\sim 180 \mu\text{g/g}$ (RT69) corresponding to ≤ 10 % lower values than the expected Nb concentration (Table 2). The match of average and expected values

Table 2 Result of mass balance, calculated values of $\mu\text{g/g}$ trace element content in titanite from point analyses, assuming closed system conditions

| Run # | Rutile starting material | Titanite theoretical value Cr | Number of all analyses (n) | Average All analyses included ($\mu\text{g/g}$) | (n) analyses $\leq 1,000$ ($\mu\text{g/g}$) | Average ($\mu\text{g/g}$) | Average ($\mu\text{g/g}$) |
|-------|--------------------------|-------------------------------|----------------------------|---|---|--------------------------------|-----------------------------|
| RT41 | 2,000 $\mu\text{g/g}$ Cr | 800 ($\mu\text{g/g}$) | 93 | 800 | 83 | 720 | |
| RT42 | | | 75 | 850 | 60 | 740 | |
| RT50 | | | 49 | 650 | 43 | 560 | |
| RT51 | | | 51 | 770 | 45 | 650 | |
| | | Theoretical value Nb | | | ≤ 250 ($\mu\text{g/g}$) | ≤ 500 ($\mu\text{g/g}$) | |
| RT49 | 500 $\mu\text{g/g}$ Nb | 200 ($\mu\text{g/g}$) | 71 | 370 | 25 | 200 | 58 |
| RT69 | | | 143 | 400 | 100 | 180 | 132 |
| RT74 | | | 48 | 990 | 9 | 190 | 27 |

appears to be excellent; however, in runs RT49 and RT74, the 25 % overstep criterion excludes a significant number of analyses, and among them a number of analyses that exceed the Nb contents of the rutile source (Fig. 1d). The run with the highest number of analyses ($n = 143$; RT69) shows a rather robust Nb distribution: 100 analyses meet the criterion $<250 \mu\text{g/g}$ Nb and yield an average $\sim 180 \mu\text{g/g}$. If 32 analyses between 250 and $500 \mu\text{g/g}$ are included, the average is $\sim 210 \mu\text{g/g}$. Including 11 analyses >500 up to $6,900 \mu\text{g/g}$ (all 143 analyses) yields an average of $\sim 400 \mu\text{g/g}$, that is, $<10\%$ 'outliers' nearly double the average Nb if included in the calculation (Table 2). Compared with RT69, the titanite analyses of RT74 show a similar, in run RT49 a smaller range of Nb content. Similarly as for Cr, we assume that Nb from the rutile is almost quantitatively included in the titanite. A rigorous mass balance of Cr and especially Nb in titanite is hampered by (1) biased statistics of a small number of analyses and by non-representative analyses in a single 2D section in samples with heterogeneous zoning and (2) the sequestration of Cr and Nb in areas with extremely high contents. A resolution of this problem would require more analyses of different sections or bulk analyses of the titanite overgrowth. The key result that the distribution of Cr and Nb in titanite is strongly variable on the μm scale is not affected by the ambiguity in the mass balance calculations.

In experiments with natural rutile, average Nb contents in titanite commonly scatter to values higher and lower than the values expected from Nb contents of adjacent rutile and average Nb concentrations in profiles vary by a factor of up to 4 in the same run (RT20; Fig. 3). The tendency that average Nb concentrations in titanite vary systematically with the Nb concentrations in adjacent rutile (Fig. 3) indicates local redistribution of Nb. Homogenization of the Nb into the bulk fluid did not occur. The strong variation of Nb in the rutile inhibits any mass balance approach (Fig. 3).

Profiles of Cr and Nb contents perpendicular to the contact rutile–titanite show no systematic zoning in titanite. We have made the same observation for Al–Ti (–F) contents in titanite (Lucassen et al. 2010b). Important variables, which commonly contribute to compositional zoning in minerals, such as P – T , the bulk composition of the system and f_{O_2} are fixed by the experimental setup and the compositions of the element sources are uniform if synthetic rutile is used. Starting materials remain present throughout the experiment and indicate phase saturation. The assemblage in the outer capsule dominates the composition of the bulk fluid and the latter should be near to saturation as indicated by quench composition, transport crystals of wollastonite, corundum, quartz by dissolution–precipitation. Differences between the runs such as the saturation of SiO_2 or Al_2O_3 or presence of F result in variable Ca–Si–Al proportions in the bulk fluid, which obviously influence the maximum substitution of Al for Ti in the titanite (Fig. 1a, d; Lucassen et al. 2010b), but the patchy zoning of the trace elements (and of Al) persists.

Major element variability in titanite influences the bond length and site volume. The volume of both the octahedral site and $^{\text{vii}}\text{Ca}$ decreases linearly with increasing Al substitution for Ti (Oberti et al. 1991). Therefore, trace element distribution might be controlled by changing crystal lattice parameters. Substitution in the experimentally formed titanite of Al^{3+} , Cr^{3+} and Nb^{5+} restricts to the $^{\text{vi}}\text{Ti}^{4+}$ site; the $^{\text{vii}}\text{Ca}^{2+}$ site could be substituted by Na^+ , but Na was never detected. However, the absence of correlations of Cr or Nb with Al precludes a control of trace element distribution by change of crystal lattice parameters during substitution of Ti by Al. Furthermore, small-scale ($<10 \mu\text{m}$ considering distances of spot analyses) heterogeneity of trace element contents occurs also in titanite without Al.

We conclude that the compositional variability of Nb and Cr must have been caused by variable availability of

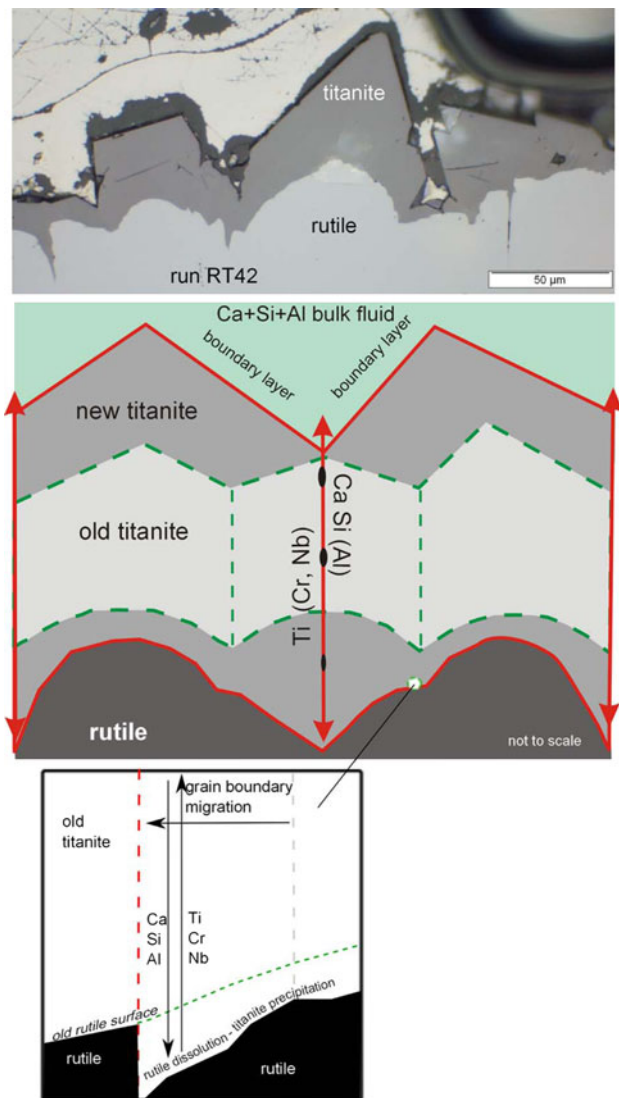


Fig. 4 Typical pattern of titanite overgrowth on rutile and transport paths for elements from the rutile source. **a** Photomicrograph in reflected light; 2D section of run RT42. The originally polished rutile surface was reshaped by titanite growth. Rutile dissolution occurs preferentially beneath grain boundaries of titanite; the zig-zag pattern of the rutile surface beneath the titanite reflects former growth stages of the titanite. **b** Scheme of titanite growth with transport pathways. Cr–Nb–Ti are transported from the rutile to the titanite–bulk fluid interface. The patchy Al zoning requires a boundary layer between titanite and bulk fluid; the compositions of boundary layer and bulk fluid are different. **c** Dissolution of rutile, titanite growth, grain boundary migration and element transport in both directions on the grain boundary occur concomitantly

the respective elements at the spot of titanite growth. The availability of these elements is controlled by transport from the rutile crystal within the titanite rim, whereas Ca and Si (and Al) are delivered by the bulk fluid (see Fig. 4). Effects of solid-state diffusion for large cations in titanite at 600 °C and the given time scale are negligible (Cherniak 2006). Our experimental study of dissolution patterns on

rutile beneath evolving titanite overgrowth (Lucassen et al. 2012) demonstrated that (1) the access to the Ti (Nb, Cr) source is canalized along titanite–titanite grain boundaries through the titanite rim; (2) titanite crystals grow by grain boundary migration and therefore the spatial configuration of transport paths changes during the runs. Sites of titanite growth are the crystal interfaces and the bulk fluid–titanite interface (Fig. 4). The importance of local element transport from the rutile along grain boundaries is corroborated by the correlation of Nb concentration in titanite with variable Nb concentrations in their substrate, the zoned natural rutile (Fig. 3). The irregular compositional zoning in the titanite precludes a systematic transport gradient of Nb, Cr, Ti and Al, for example, related to the distance to the rutile or bulk fluid. The driving mechanism behind the build-up of different element concentrations and growth of compositionally different domains in the crystals is not understood, but obviously bound to the specific spatial relations of the element sources and restricted access via grain boundaries.

Relevance for natural rutile–titanite assemblages

Trace element contents of titanite overgrowths on rutile and vein-grown large single-crystal titanite without relations to precursor rutile in a retrogressed eclogite was studied in detail (Lucassen et al. 2010a, 2011). The retrograde titanite growth occurred at amphibolite facies temperatures and formed a complete overgrowth on rutile, which was consumed to different extent by titanite. Natural and experimental titanite on rutile show similar elemental zoning (Lucassen et al. 2010b, 2011) and dissolution pattern on the rutile surface (Lucassen et al. 2012). Element transport paths (Fig. 4) in the natural titanite overgrowth were similar as those in the experiments according to the dissolution patterns on the rutile (Lucassen et al. 2012). In this sample, the scatter of Nb contents (from ~40 to ~180 µg/g; Fig. 5a) and other HFSE elements in titanite on rutile is considerable and shows no systematic distribution. Variable Al and HFSE contents are not correlated, and Al zoning in the titanite is irregular. In contrast, the large single-crystal titanite in a vein has lower and uniform HFSE contents, analysed in a core-rim profile (Fig. 5a), and the spatial distribution of variations of the HFSE concentrations appears to be related to changes in the composition of the vein fluid. The composition of the vein fluid represents a larger rock volume, whereas Nb (also Ta and W; Lucassen et al. 2011) in the titanite overgrowths comes from the rutile precursor and is likely distributed by elemental transport along titanite grain boundaries. Interestingly, strongly variable concentrations of other trace elements (e.g., Sr, U, Pb, REE) that are brought from an external source via fluid to the titanite show a good to fairly

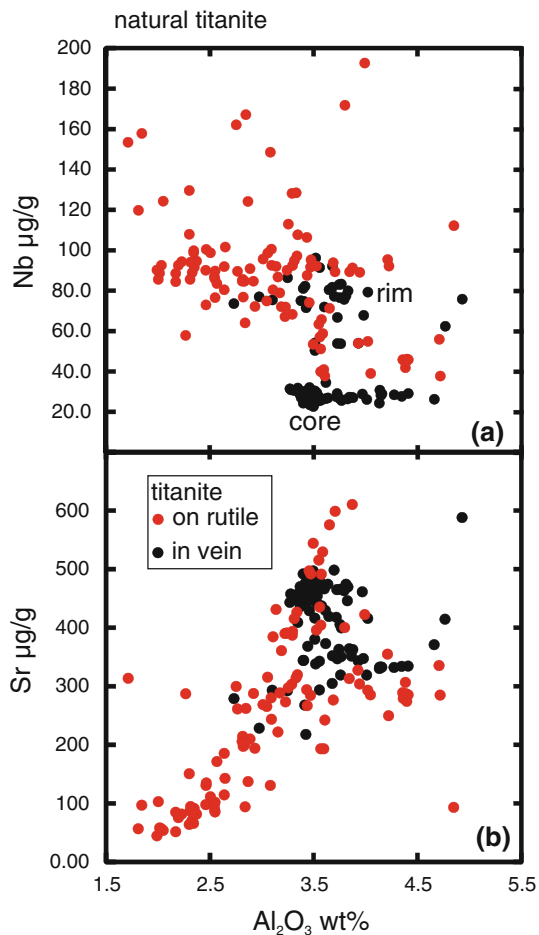


Fig. 5 Titanite composition from an amphibolite, retrogressed from eclogite. **a** Niobium and Al contents of titanite overgrowths on rutile (red dots) cover a wide range and the spatial distribution is irregular; titanite in a vein (black dots, core and rim) has a much more restricted range of Nb and Al contents. **b** Content of Al and Sr in the titanite on rutile, with large scatter, compared to titanite in the vein. The positive correlation of Al and Sr contents indicates a fairly uniform composition of the fluid from the rock matrix

good positive correlation with the Al contents of titanite (Fig. 5b). This means that the composition of the Al-bearing fluid is fairly constant and likely buffered by the mineral assemblage of the rock, but the amount of Ti (and related trace elements) incorporated in the titanite is controlled locally by the transport growth mechanism in and around the titanite.

We conclude from observation of the experimentally and natural titanite overgrowth on rutile that the compositional zoning is due to the availability of elements at the site of growth in the titanite. This is strongly influenced by the extent of elemental transport within the titanite rim between the inner (rutile) source and the outer source (fluid from the rock matrix in nature or bulk fluid in our experiments). Such zoning allows no direct clues, for example,

on changes of P – T or on the possibly changing composition of open systems.

Acknowledgments We thank Christa Zecha, Technische Universität Berlin (TUB) for sample preparation and Oona Appelt for help with the microprobe at Deutsches Geoforschungszentrum (GFZ); Peter Dulski (GFZ) for LA-ICP-MS analyses of the synthetic rutile, Helga Kemnitz and Ilona Schäpan (both GFZ) and Jörg Nissen (Zentraleinrichtung Elektronenmikroskopie, TUB) for their help with the SEM, Irene Preuß (TUB) for help with microphotography. Thomas Fockenberg (Ruhr-Universität Bochum) kindly supplied grossular from Namibia as a starting material for the experiments. We thank Peter Tropper and an anonymous reviewer for their comments that improved the manuscript. This work was carried out as part of the research group FOR 741 ‘Nanoscale processes and geomaterials properties’, sponsored by DFG code number DR DFG grant DR 744/3-1 and grant FR 557/26-2.

References

- Antignano A, Manning CE (2008) Rutile solubility in H_2O , H_2O – SiO_2 , and H_2O – $NaAlSi_3O_8$ fluids at 0.7–2.0 GPa and 700–1000 C: implications for mobility of nominally insoluble elements. *Chem Geol* 255:283–293
- Aranovich LY, Newton RC (1996) H_2O activity in concentrated NaCl solutions at high pressures and temperatures measured by the brucite-periclase equilibrium. *Contrib Mineral Petrol* 125:200–212
- Ayers JC, Watson EB (1993) Rutile solubility and mobility in supercritical aqueous fluids. *Contrib Mineral Petrol* 114:321–330
- Bea F, Montero P, Ortega M (2006) A LA-ICP-MS evaluation of Zr reservoirs in common crustal rocks: implications for Zr and Hf geochemistry and zircon-forming processes. *Can Mineral* 44:693–714
- Bernau R, Franz G (1987) Crystal chemistry and genesis of Nb-, V-, and Al-rich metamorphic titanite from Egypt and Greece. *Can Mineral* 25:695–705
- Brewer TS, Storey CD, Parrish RR, Temperley S, Windley BF (2003) Grenvillian age decompression of eclogites in the Glenelg-Attadale Inlier, NW Scotland. *J Geol Soc London* 160:565–574
- Cherniak DJ (2006) Zr diffusion in titanite. *Contrib Mineral Petrol* 152:639–647
- Connolly JAD (1990) Multivariable phase-diagrams—an algorithm based on generalized thermodynamics. *Am J Sci* 290:666–718
- Connolly JAD (2009) The geodynamic equation of state: what and how. *Geochem Geophys Geosyst* 10:Q10014. doi:10.1029/2009GC002540
- Fockenberg T, Burchard M, Maresch WV (2008) The solubility of natural grossular-rich garnet in pure water at high pressures and temperatures. *Euro J Mineral* 20:845–855
- Frost BR, Chamberlain KR, Schumacher JC (2000) Sphene (titanite): phase relations and role as a geochronometer. *Chem Geol* 172:131–148
- Fulmer EC, Nebel O, van Westrenen W (2010) High-precision high field strength element partitioning between garnet, amphibole and alkaline melt from Kakanui, New Zealand. *Geochim Cosmochim Acta* 74:2741–2759
- Fyfe WS, Price NJ, Thompson AB (1978) *Fluids in the earth's crust*. Elsevier, Oxford, NY, p 383
- Grew ES, Yates MG, Wilson CJL (2008) Aureoles of Pb(II)-enriched feldspar around monazite in paragneiss and anatectic pods of the Napier Complex, Enderby Land, East Antarctica: the roles of

- dissolution-precipitation and diffusion. *Contrib Mineral Petrol* 155:363–378
- Groat LA, Carter RT, Hawthorne FC, Ercitt TS (1985) Tantalian niobian titanite from the Irgon Claim, southeastern Manitoba. *Can Mineral* 23:569–571
- Hayden LA, Watson B, Wark DA (2008) A thermobarometer for sphene (titanite). *Contrib Mineral Petrol* 155:529–540
- Kohn MJ (2003) Geochemical zoning in metamorphic minerals. In: Rudnick R (ed) *Treatise on geochemistry*, vol 3. The crust. Elsevier, pp 229–261
- Konrad-Schmolke M, O'Brien PJ, Heidelbach F (2007) Compositional re-equilibration of garnet: the importance of sub-grain boundaries. *Euro J Mineral* 19:431–438
- Lucassen F, Dulski P, Abart R, Franz G, Rhede D, Romer RL (2010a) Redistribution of HFSE elements during rutile replacement by titanite. *Contrib Mineral Petrol* 160:279–295
- Lucassen F, Franz G, Rhede D, Wirth R (2010b) Ti-Al zoning of experimentally grown titanite in the system CaO-Al₂O₃-TiO₂-SiO₂-NaCl-H₂O-(F)—evidence for small scale fluid heterogeneity. *Am Mineral* 95:1365–1378
- Lucassen F, Franz G, Dulski P, Romer RL, Rhede D (2011) Element and Sr isotope signatures of titanite as indicator of variable fluid composition in hydrated eclogite. *Lithos* 121:12–24
- Lucassen F, Franz G, Wirth R, Weise M, Hertwig A (2012) The morphology of the reaction front of the dissolution-precipitation reaction rutile + wollastonite = titanite in time series experiments at 600 °C/400 MPa. *Am Mineral* 97:828–839
- Martin AJ (2009) Sub-millimeter heterogeneity of yttrium and chromium during growth of semi-pelitic garnet. *J Petrol* 50:1713–1727
- Meinhold G (2010) Rutile and its applications in earth sciences. *Earth Sci Rev* 102:1–28
- Newton RC, Manning CE (2006) Solubilities of corundum, wollastonite and quartz in H₂O–NaCl solutions at 800 °C and 10 kbar: interaction of simple minerals with brines at high pressure and temperature. *Geochim Cosmochim Acta* 71:5571–5582
- Oberti R, Smith DC, Rossi G, Caucia F (1991) The crystal chemistry of high-aluminum titanites. *Eur J Mineral* 3:777–792
- Pouchou JL, Pichoir F (1985) 'PAP' (Z) procedure for improved quantitative microanalysis. *Microbeam Anal* 1985:104–106
- Rapp JF, Klemme S, Butler IB, Harley SL (2010) Extremely high solubility of rutile in chloride and fluoride-bearing metamorphic fluids: an experimental investigation. *Geology* 38:323–326
- Ribbe PH (1980) Titanite. In: Ribbe PH (ed) *Orthosilicates: reviews in mineralogy*, vol 5. Mineralogical Society of America, Washington, pp 137–154
- Romer RL, Rötzler J (2003) Effect of metamorphic reaction history on the U–Pb dating of titanite. In: Vance D (ed) *Geochronology: linking the isotopic record with petrology and textures*, vol 220. Geological Society Special Paper, pp 147–158
- Schmidt A, Weyer S, John T, Brey GP (2009) HFSE systematics of rutile-bearing eclogites: new insights into subduction zone processes and implications for the Earth's HFSE budget. *Geochim Cosmochim Acta* 73:455–468
- Smith MP, Storey CD, Jeffries TE, Ryan C (2009) In situ U–Pb and trace element analysis of accessory minerals in the Kiruna District, Norrbotten, Sweden: new constraints on the timing and origin of mineralization. *J Petrol* 50:2063–2094
- Storey CD, Smith MP, Jeffries TE (2007) In situ LA-ICP-MS U–Pb dating of metavolcanics of Norrbotten, Sweden: records of extended geological histories in complex titanite grains. *Chem Geol* 240:163–181
- Tropper P, Manning CE (2008) The current status of titanite–rutile thermobarometry in ultrahigh-pressure metamorphic rocks: the influence of titanite activity models on phase equilibrium calculations. *Chem Geol* 254:123–132
- van der Laan SR, van Groos AFK (1991) Pt-Fe alloys in experimental petrology applied to high-pressure research on Fe-bearing systems. *Am Mineral* 76:1940–1949
- Zack T, Kronz A, Foley SF, Rivers T (2002) Trace element abundances in rutiles from eclogites and associated garnet mica schists. *Chem Geol* 184:97–122
- Zack T, Moraes R, Kronz A (2004) Temperature dependence of Zr in rutile: empirical calibration of a rutile thermometer. *Contrib Mineral Petrol* 148:471–488